Vol. 569: 89–102, 2017
https://doi.org/10.3354/meps12072

MARINE ECOLOGY PROGRESS SERIES
Mar Ecol Prog Ser

Published April 7

Microbial food web structure and dynamics across a natural temperature gradient in a productive polar shelf system

Gayantonia Franzè[1,2], Peter J. Lavrentyev[1,*]

[1]The University of Akron, Department of Biology, Akron, OH 44325, USA

[2]*Present address:* University of Rhode Island, Graduate School of Oceanography, Narragansett, RI 02882, USA

ABSTRACT: Recent rapid climate change in the Arctic has profound effects on polar marine ecosystems. In this study, we used time-for-space substitution to evaluate possible plankton responses to sea ice reduction and rising sea temperatures. The microbial food web was examined across a natural temperature gradient in the Barents Sea and adjacent waters (70–78.5°N; −1.8 to 8.6°C) during different seasonal phases. On average, grazers consumed 92% of phytoplankton daily production (57 and >100% in the ice-covered Arctic and the North Atlantic-influenced open waters, respectively). Microzooplankton biomass and production peaked on the Atlantic side of the Polar Front, where mixotrophic ciliates were responsible for up to 49% of total chlorophyll *a* and a very efficient energy transfer (community production to ingestion ratios of 38 to >100%). Despite pronounced seasonal and latitudinal shifts in plankton composition, several key microbial food web parameters increased linearly with temperature, including bacterial biomass, microzooplankton herbivory rate and its relative impact, and the proportion of smaller and heterotrophic cells in microzooplankton. Overall, the microbial food web changed gradually across the temperature gradient and was characterized by tight trophic linkages among its constituents within the dominant water masses.

KEY WORDS: Barents Sea · Microzooplankton · Herbivory · Bacteria · Secondary production · Dilution assay · Temperature effect

Resale or republication not permitted without written consent of the publisher

INTRODUCTION

Global climate change disproportionally affects polar regions (Stocker et al. 2013), where average temperatures have risen 3 times the global average (Polyakov et al. 2010). The Barents Sea, one of the most productive polar shelf ecosystems (Ellingsen et al. 2008, Hunt et al. 2013), has been warmer in the last decade than over the previous 110 yr of observation (Boitsov et al. 2012) and has experienced an increase in heat transport from the Atlantic Ocean (Arthun et al. 2012). Significant losses of sea ice (Kwok & Rothrock 2009) and a longer open-water season in the Arctic (Arrigo & van Dijken 2011) have already led to increased pelagic primary production (Slagstad et al. 2011, Brown & Arrigo 2012) with a larger contribution of small-sized phytoplankton (Li et al. 2009). These changes are expected to bolster the pelagic system at the expense of the benthic components, with profound impacts on trophic structure and carbon fluxes (Wassmann & Reigstad 2011, Wassmann & Lenton 2012). Therefore, the immediate fate of primary production can be as critical as its amount in polar ecosystems, where higher trophic levels depend on efficient energy transfer (McBride et al. 2014), and even minor climate effects at the base of food webs can be amplified through trophic chains (Sarmento et al. 2010).

The main goal of our study was to examine microbial dynamics in the rapidly changing Barents Sea environment with emphasis on the top trophic level within the microbial food web, microzooplankton.

*Corresponding author: peter3@uakron.edu

© Inter-Research 2017 · www.int-res.com

Microzooplankton grazing is a main conduit for pelagic primary production and bacterial carbon recovered through the microbial loop in the ocean (Calbet & Landry 2004, Caron & Hutchins 2013). The hypothesized selective stimulating effect of higher temperature on the growth of heterotrophic protists is likely to increase their importance as trophic intermediaries (Rose & Caron 2007) and counterbalance increased primary production (Chen et al. 2012). Based on these predictions, Hypothesis 1 (*H*1) of our study was that microzooplankton herbivory and its relative impact on primary production will increase with temperature. At the same time, polar microzooplankton intrinsic growth is not constrained by low temperatures more than that of phytoplankton (Franzè & Lavrentyev 2014). Further, polar protist ingestions rates may be temporarily decoupled from their growth (Rose et al. 2013). Therefore, our first null hypothesis ($H1_0$) was that temperature will have little or no effect on microzooplankton herbivory rates and impact.

A 3D model of the Barents Sea ecosystem attaches much importance to the microbial food web in ice-free waters (Wassmann et al. 2006a). Its assumptions are based on the dominance of small-sized phytoplankton in summer (Rat'kova & Wassmann 2002, Not et al. 2005, Druzhkova & Makarevich 2008, Reigstad et al. 2011), elevated heterotrophic microbial biomass (Hansen et al. 1996, Howard-Jones et al. 2002, Rat'kova & Wassmann 2002), and microzooplankton herbivory rates measured along a single north–south transect in July (Verity et al. 2002). These observations led to *H*2 that microzooplankton capacity to control phytoplankton growth will increase in ice-free waters. This prediction is not self-evident, as microzooplankton in general, and dinoflagellates in particular, are known to feed voraciously on large diatoms (e.g. Strom & Fredrickson 2008, Sherr et al. 2013), which dominate in the marginal ice zone. $H2_0$ was therefore that we would find no difference between herbivory in ice-covered and open waters in terms of microzooplankton grazing.

The dynamics of Barents Sea plankton community subjected to experimentally elevated temperatures indicated a thermal threshold around 5 to 6°C beyond which plankton community metabolism became net heterotrophic (Holding et al. 2013). In addition, experimental warming led to the replacement of dominant diatoms by the pico-prasinophyte *Micromonas* and nano-flagellates (Coello-Camba et al. 2015). If similar thresholds occur under natural conditions, the associated changes within the microbial food web could cascade to its top trophic level, microzooplankton, with potential consequences for the entire pelagic ecosystem. Our *H*3 was that microbial food web structure and dynamics will undergo an abrupt change >5°C. Temperature-shift experiments have been criticized for having limited predictive power for long-term adaptations (Kirchman et al. 2009, Tatters et al. 2013), as the sudden change in temperature affects plankton in ways fundamentally different from those likely to be experienced in reality (Sarmento et al. 2010). $H3_0$ was thus that there would be no temperature thresholds for microbial food web dynamics and structure within the Barents Sea ambient range.

Apart from expensive and logistically challenging long-term observations, the only other way to assess polar plankton responses to habitat changes over time is through a substitution of space for time. In this approach, diverse habitats across space are compared to gauge possible future changes in the Arctic (Nelson et al. 2014). Using this approach, we examined the structure and dynamics of natural microbial plankton communities across a natural temperature gradient during 3 critical phases in the seasonal cycle: early bloom, late bloom, and post-bloom. As an interface between the Atlantic and Arctic Oceans, the Barents Sea shelf provides an ideal place for examining plankton communities that are adapted to different environments. It is the only Arctic region that remains ice-free throughout the year up to 74–75° N (Smolyar & Adrov 2003) due to the inflow of the Atlantic Drift from the southwest. In the north, cold Arctic Water (AW) flows through the opening between Spitsbergen, Franz Josef Land, and Novaya Zemlia and meets relatively warm North Atlantic Water (NAW), forming a distinct Polar Front (PF, Nikiforov & Shpaikher 1980). Above the PF, the diatom bloom occurs in May in the marginal ice zone and follows the receding ice edge, whereas the NAW section exhibits a single vernal bloom followed by secondary wind-driven peaks in production (Qu et al. 2006, Sakshaug et al. 2009). Once nutrients accumulated during the winter and released from the melting ice have been exhausted, a deep chlorophyll *a* maximum (DCM) forms near the pycnocline.

MATERIALS AND METHODS

Twenty shipboard incubation experiments were conducted in May 2010, August to September 2010, and June 2011 during 3 expeditions, which crossed the PF from NAW in the south to AW in the north (Fig. 1, and see Table 1). The locations of the main water masses were determined from temperature

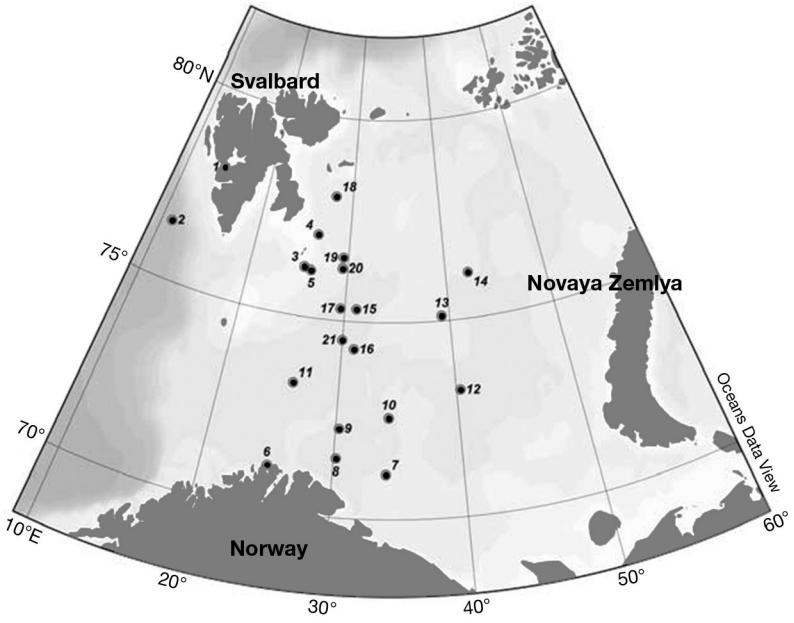

Fig. 1. Experimental locations in the Barents Sea. See Table 1 for environmental conditions during each experiment. Experiment numbering corresponds to Franzè & Lavrentyev (2014)

and salinity (Loeng 1991, Vage et al. 2014). The May and June cruises also included the marginal ice zone and seasonal sea ice floes between Hopen Island and Kong Karls Land. In May 2010, 1 experiment (Expt 1) was conducted in Isfjorden, Spitsbergen, which is influenced by AW.

At each station, seawater temperature, salinity, and raw fluorescence were measured using a Seabird 911 Plus CTD system equipped with a fluorometer. Seawater was collected in 5 l Niskin bottles from the DCM, carefully syphoned into a 20 l polycarbonate carboy using submerged silicone tubing, and immediately transported to a shipboard temperature-controlled cold room (±1°C ambient sea temperature), where all manipulations were conducted under dim light. The collected seawater was added to triplicate 0.6 l Nalgene clear glass bottles. To avoid damaging delicate microzooplankton (Gifford 1985) and altering phytoplankton composition, the samples were not screened prior to incubation (Calbet et al. 2011a, Sherr et al. 2013). Instead, larger zooplankton were removed using a long glass pipette. Post-incubation screening indicated that this technique was effective in removing mesozooplankton.

Phytoplankton growth and grazing loss rates were determined in 2-point dilution assays (Landry et al. 2008), where the grazing rate (g) was calculated as the difference in prey growth (μ) in undiluted and highly diluted treatments. We selected this approach because it provides the same growth and grazing rate estimates as the original multi-point approach (Strom & Fredrickson 2008) but is more efficient and less affected by uncertainty in changes in microzooplankton clearance and growth rates, and trophic interactions across a dilution gradient (Dolan et al. 2000, First et al. 2007, Calbet & Saiz 2013). In addition, 2 concurrent microzooplankton studies in the Bering Sea (Sherr et al. 2013, Stoecker et al. 2014a) also relied on the 2-point method and provided a base for comparison.

The diluted treatments were prepared by mixing 9 parts filtered seawater (0.2 µm large volume Pall Science pleated capsules using gravity flow) with 1 part whole seawater to yield a 10% dilution. The capsules were presoaked in 5% HCl and thoroughly rinsed with deionized water prior to use. To equalize plankton growth conditions, all samples except for the whole seawater controls were amended with dissolved nutrients to final concentrations of 16 µM N (KNO_3 + NH_4Cl; 15:1 based on N) and 1 µM P (K_2HPO_4).

All bottles were screened with neutral density filters to mimic 25% surface irradiance and incubated in a deck incubator with running surface seawater for 24 h. During most experiments, temperature remained within ± 0.5°C of the initial sea temperature. The only exception was Expt 16 in September 2010, when temperatures increased from 4.6 to 9.0°C due to an unexpected early call in port. In May 2010, the incubator included a plankton wheel; during the other 2 cruises, bottles were rotated periodically by hand.

Plankton samples were collected at T_0 and T_{24}. For chlorophyll *a* (chl *a*) analysis, between 250 and 500 ml of seawater were filtered onto 0.2 µm nylon membrane filters, shock-frozen, and stored in liquid N_2. Phytoplankton and bacterial samples were preserved with 0.2 µm-filtered formaldehyde (1% final concentration) and frozen in liquid N_2. Microzooplankton samples were preserved in 2% (final concentration) acid Lugol's iodine, post-fixed with 1% (final concentration) formaldehyde after 24 h, and stored at 4°C. Additional plankton samples were fixed with 1% (final concentration) formaldehyde for phytoplankton and heterotrophic nanoflagellate (HNF) counts and stored at 4°C.

Chl *a* was extracted in 90% acetone for 24 h at –20°C and measured fluorometrically using the nonacidic method (Welschmeyer 1994). Phototrophic picoplankton was counted using a Partec CyFlow SL flow cytometer with 1 µm inert beads added as a reference. Bacteria were counted after staining with

SYBR Green I (Marie et al. 1997). The cell size of at least 2000 DAPI-stained (Porter & Feig 1980) bacterial cells was determined per sample using an image analysis system, which consisted of an epifluorescent microscope (1000×), a high-resolution digital camera, and Image Pro Plus software (Media Cybernetics). Bacterial volumes were then converted to carbon (Norland 1993).

Phytoplankton size structure was characterized in Expts 1 to 12 using an imaging-in-flow system (FlowCAM; Sieracki et al. 1998). Samples were processed in the cell-triggered mode (emission >650 nm), and the flow rate and particle concentrations were adjusted to capture 1 particle of interest per frame on average. Biovolumes of single cells were calculated using their automatically measured linear dimensions, whereas chain-forming diatoms were counted as whole particles, and their volumes were determined automatically based on areal diameter (Jakobsen & Carstensen 2011). In addition, in Expts 3, 4, 7, and 16, phytoplankton were counted and sized via microscopy.

Microzooplankton were settled onto Utermöhl chambers (50–100 ml) and counted under an inverted microscope equipped with differential interference contrast (DIC) and fluorescence. The entire surface area of a chamber was scanned at 200×. At least 40 individual cells within each abundant taxon were sized with an eyepiece micrometer at 400–600× and converted to carbon based on approximated geometric shapes and volume to carbon conversions (Putt & Stoecker 1989, Menden-Deuer & Lessard 2000). All ciliates were included in microzooplankton, whereas dinoflagellates <20 µm in maximum dimension were allocated to nanoplankton (Møller et al. 2006). Ciliates and dinoflagellates were examined for chloroplasts in formaldehyde-preserved samples using DIC and chl *a* autofluorescence and allocated into heterotrophs and mixotrophs (i.e. pigmented ciliates and dinoflagellates). Mixotrophic chl *a* content was calculated based on their volume (Montagnes et al. 1994), assuming that the volume to chl *a* relationship is similar to that in autotrophic plankton (Dolan & Perez 2000). HNF were counted using black 0.8 µm filters, DAPI, and an epifluorescent microscope at 500 to 1000× as described above. Cells were examined for the presence of flagella and chl *a* autofluorescence, and biomass was calculated based on Menden-Deuer & Lessard (2000).

Prey apparent growth rates were calculated assuming exponential growth: $\mu = \ln(N_t/N_0)/(t/24)$, where: μ = growth rate (d^{-1}), N_0 and N_t = prey abundance at the beginning and end of the experiment, respectively, and t = time (h). Grazing mortality rates (g) were determined as the difference between μ measured in the diluted ($\mu_{10\%}$) and whole (μ_{WSW}) seawater samples: $g = \mu_{10\%} - \mu_{WSW}$. The percentage of the initial standing stocks of prey removed by grazers was calculated as $\{[(C_0e^{\mu} - C_0) - (C_0e^{(\mu-g)} - C_0)]/C_0e^{\mu}\} \times 100$, where C_0 is prey abundance or concentration (µg chl l^{-1}), at time zero in the whole seawater treatments (Anderson & Rivkin 2001). In the experiments where prey grew slower in diluted samples, or were not significantly different from the whole seawater treatment, g was not calculated and is reported as 0 (Stoecker et al. 2014a), whereas the growth of prey was reported from the whole seawater treatment. If prey concentrations declined in all treatments, their growth was also reported as 0.

Microzooplankton community secondary production (MzP, µg C l^{-1} d^{-1}) was calculated by summing the secondary production of individual taxa (Nielsen & Kiørboe 1994, Levinsen et al. 1999), which was calculated from their initial population biomass (b_0, µg C l^{-1}) and the instantaneous growth rates (r, d^{-1}) observed in the simultaneous experiments (Franzè & Lavrentyev 2014): $MzP = \Sigma\ r \times b_0$. The microzooplankton community daily specific growth rate was then calculated by dividing production by total initial community biomass (B_0): $MzP/B = MzP/B_0$. The percentage of growing microzooplankton was calculated as the ratio between the initial biomasses of microzooplankton that grew during a given incubation and total microzooplankton.

Standard deviation was used as a measure of dispersion throughout the study. Differences between diluted and undiluted samples were analyzed using a 2-tailed t-test assuming unequal variances and among microbial parameters in different water masses using ANOVA and Fisher's LSD test. Relationships between plankton characteristics and water temperature were examined using Pearson correlation and least square linear regression. All statistical analyses were conducted using Minitab 17.

RESULTS

Environmental data

Ambient sea temperatures varied between –1.8 and 8.6°C (Table 1) and showed a strong latitudinal trend ($r = 0.93$, $p < 0.005$), which was little affected by seasonality. Five stations had temperature and salinity typical for AW (–1.3 ± 0.22°C and 34.4 ± 0.20, respectively); 4 of them were ice-covered, whereas Isfjorden

Table 1. Environmental conditions during the experiments. Expt 2 (Franze & Lavrentyev 2014, see our Fig. 1) was conducted in the Greenland Sea and, therefore, is not included in this paper. AW: Arctic Water; NAW: North Atlantic Water; PF: Polar Front; CW: Coastal Water; Chl: chlorophyll *a*. Dates are given as dd/mm/yy

Expt	Date	Temp. (°C)	Salinity	Depth (m)	Water mass	Ice	Chl (µg l^{-1})
1	04/05/10	−1.3	34.4	17	AW-Fjord	No	1.64
3	07/05/10	−1.3	34.6	10	AW	Yes	3.19
4	08/05/10	−1.8	34.4	2	AW	Yes	3.52
5	09/05/10	0.3	34.9	35	AW-PF	No	1.37
6	24/08/10	8.6	34.3	10	NAW-CW	No	1.91
7	26/08/10	7.2	34.7	10	NAW-CW	No	1.82
8	27/08/10	7.4	34.8	30	NAW-CW	No	1.58
9	30/08/10	7.5	35.0	20	NAW	No	1.20
10	01/09/10	5.6	35.0	10	NAW	No	1.77
11	02/09/10	7.0	35.1	25	NAW	No	0.79
12	04/09/10	4.2	34.6	20	NAW-PF	No	2.18
13	07/09/10	3.1	34.7	20	NAW-PF	No	0.67
14	09/09/10	2.4	34.7	20	NAW-PF	No	0.38
15	10/09/10	4.9	35.1	20	NAW	No	0.10
16	12/09/10	4.6	35.1	20	NAW	No	1.61
17	21/06/11	4.0	35.1	35	NAW	No	1.86
18	22/06/11	−1.8	34.1	30	AW	Yes	5.19
19	24/06/11	−0.5	34.5	44	AW	Yes	1.32
20	26/06/11	0.0	34.7	38	AW-PF	No	1.37
21	27/06/11	4.0	35.9	20	NAW	No	1.44

was ice-free. Four stations on the Atlantic side and 1 on the Arctic side represented the PF (1.99 ± 1.82°C, 34.7 ± 0.10). Seven experiments were conducted in NAW (5.24 ± 1.24°C, 35.3 ± 0.31), and the 3 southernmost stations off the Finnmark coast were affected by coastal water (CW, 7.73 ± 0.76°C, 34.6 ± 0.25) to varying degrees.

Plankton community structure

In May and June, phytoplankton peaked under the ice (chl *a* up to 5 µg l^{-1}, Table 1), mostly due to large and chain-forming diatoms such as *Thalassiosira* spp., *Thalassionema* spp., *Fragilariopsis cylindrus*, *Rhizosolenia styliformis*, and *Chaetoceros* spp. In Expt 4, we also found colonies of the ice diatom *Nitzschia frigida*. Phytoplankton >50 µm ESD formed between 70 and 80% of total phytoplank-

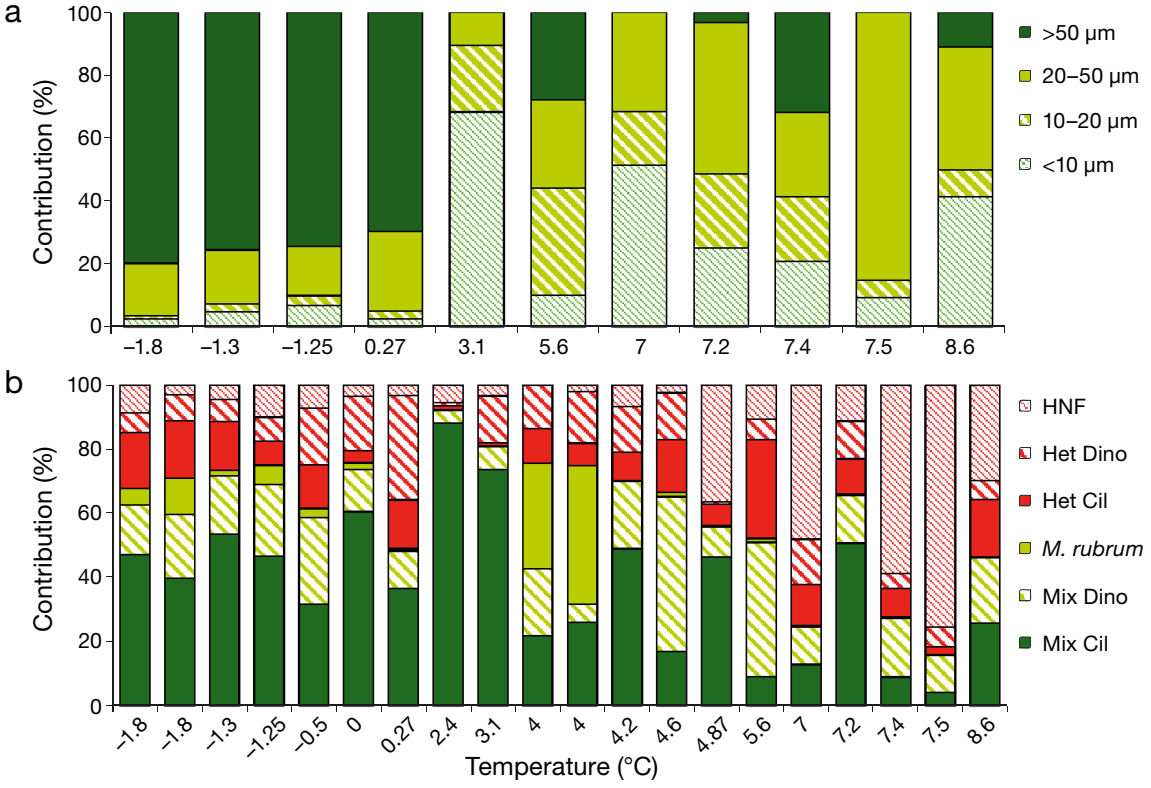

Fig. 2. (a) Phytoplankton size structure and (b) microbial grazer composition across the temperature gradient (note that data points from different locations/experiments may share the same ambient temperature). Percentages indicate contribution to total biovolume (a) and carbon-based biomass (b). Mix Cil: mixotrophic ciliates; Mix Dino: mixotrophic dinoflagellates; Het Cil: heterotrophic ciliates; Het Dino: heterotrophic dinoflagellates; *M. rubrum*: *Mesodinium rubrum*; HNF: heterotrophic nanoflagellates

ton volume in AW (Fig. 2a). In June, single cells and colonies of the haptophyte *Phaeocystis pouchetii* occurred in the marginal ice zone. In the open water, except Isfjorden, the DCM was primarily formed by smaller phytoplankton, including diatoms and cryptophyte and chrysophyte flagellates; *Micromonas* occurred in the ice-covered and open waters.

Bacterial biomass ranged from 2.5 µg C l^{-1} in May to 36.2 µg C l^{-1} in June, with both extreme values recorded under the ice (Tables 1 & 2). In the open waters, bacterial biomass increased with temperature ($r = 0.67$; $p < 0.005$) due to both their abundance and cell volume (Table 2). The HNF abundance (0.05 and 0.98 × 10^6 cell l^{-1}) mostly consisted of chrysophytes, with minor contributions from choanoflagellates and bodoniids. HNF biomass (0.38 to 5.49 µg C l^{-1}) increased with temperature ($r = 0.77$; $p < 0.005$) and was dominated by nano-dinoflagellates and, in warmer waters, by the kathablepharid *Leucocryptos marina*. The contribution of HNF to total grazer biomass (i.e. microzooplankton + HNF) increased with temperature and reached its maximum of 75% in the warmer NAW in August (Fig. 2b, at 7.5°C). In the ice-free waters, the HNF to bacteria biomass ratio increased with temperature ($r = 0.64$, $p < 0.05$, Table 2).

Microzooplankton biomass (1.36 to 93.3 µg C l^{-1}, Table 2) peaked under the ice in May and on the Atlantic side of the PF in June and August and declined at temperatures >6°C. The microzooplankton biomass to chl *a* ratio was significantly higher at the intermediate temperatures (31:1) than in AW (10:1) and NAW >5°C (11:1, Fisher's LSD test, $p < 0.05$). The contribution of ciliates to microzooplankton biomass (Fig. 2b) mostly depended on the large mixotrophic oligotrichs *Laboea strobila*, *Strombidium conicum*, and *S. wulffi* and peaked within the PF. Plastidic *Mesodinium* cells ranged from 15 to 55 µm ESD and probably included different species (Garcia-Cuetos et al. 2012). However, the most abundant and common form was 28–35 µm ESD and fit the description of *M. rubrum*. It was present at most stations, contributing, on average, under 2% of microzooplankton biomass. In June, *M. rubrum* peaked on the Atlantic side of the PF and contributed up to 44%. Among dinoflagellates, *Gyrodinium spirale* and *Protoperidinium bipes* dominated under the ice, whereas *Gymnodinium heterostriatum*, *Dinophysis norvegica*, *Ceratium arcticum*, and *C. fusus* were common in NAW. The contribution of microzooplankton <25 µm ESD (mostly ciliates *Lohmanniella oviformis*, *Balanion comatum*, and *S. epidemum* and the dinoflagellates *Amphidinium sphenoides*, *G. arcticum*,

Table 2. Microbial parameters and their ratios at the experimental stations. Bac: bacteria; HNF: heterotrophic nanoflagellates; Mz: microzooplankton; Dino: Dinoflagellates; *M. rubrum*: *Mesodinium rubrum*; MixChl: calculated mixotrophic chlorophyll *a*; Chl: extracted chlorophyll *a*; MzP: microzooplankton secondary production; *B*: microzooplankton biomass; nd: no data. The ratios are based on biomass values

Expt	Biomass (µg C l^{-1})			Abundance (cell l^{-1})					Bac volume	HNF: Bac	Mz: Chl	MixChl: Chl	MzP: *B*
	Bac	HNF	Mz	Bac ×10^9	HNF ×10^6	Dino ×10^3	Ciliates ×10^3	*M. rubrum* ×10^3	(µm^3)				
1	9.48	1.80	16.2	0.39	0.11	2.43	4.10	0.28	0.11	0.19	9.88	8.98	0.33
3	2.50	1.03	22.2	0.13	0.05	2.00	1.66	0.10	0.08	0.41	6.95	4.46	0.27
4	3.36	1.76	18.6	0.13	0.43	2.40	2.06	0.40	0.12	0.52	5.27	3.74	0.08
5	5.24	0.38	10.9	0.21	0.09	1.60	0.91	0.01	0.11	0.07	7.97	4.21	0.07
6	16.1	4.67	11.0	0.70	0.68	1.98	2.98	0.02	0.10	0.29	5.79	3.66	0.06
7	23.2	2.49	19.6	0.69	0.27	7.26	5.18	0.04	0.17	0.11	10.79	6.76	0.09
8	12.2	5.49	3.86	0.58	0.67	1.98	1.40	0.02	0.09	0.45	2.44	2.43	0.10
9	22.1	4.18	1.36	0.97	0.98	0.66	0.58	0.00	0.10	0.19	1.14	1.13	1.60
10	32.8	3.51	29.2	0.90	0.33	5.66	4.36	0.12	0.19	0.11	16.53	15.30	0.22
11	21.8	3.39	3.66	0.84	0.51	1.66	1.90	0.02	0.12	0.16	4.61	2.96	0.14
12	24.7	1.76	24.2	0.85	0.33	1.96	2.14	0.04	0.14	0.07	11.12	14.35	0.65
13	12.5	1.23	35.2	0.41	0.10	2.96	1.58	0.00	0.15	0.10	52.41	33.25	0.08
14	9.34	1.02	17.4	0.36	0.24	0.78	1.18	0.02	0.12	0.11	45.91	27.79	0.04
15	18.7	2.26	3.96	0.72	0.52	0.78	0.54	0.02	0.12	0.12	39.57	27.91	0.04
16	17.2	0.50	19.8	0.66	0.11	4.90	4.66	0.08	0.12	0.03	12.33	13.95	0.07
17	10.4	nd	41.0	0.40	nd	2.46	5.10	2.46	0.12	nd	22.03	18.95	0.23
18	36.2	0.56	18.3	1.48	0.07	3.66	9.68	1.02	0.11	0.02	3.53	2.83	0.13
19	16.7	0.87	11.3	0.64	0.29	3.80	3.22	0.04	0.12	0.05	8.57	7.03	0.15
20	31.4	1.19	32.9	1.48	0.29	5.04	6.44	0.16	0.09	0.04	24.00	20.24	0.07
21	15.9	1.90	93.3	0.52	0.31	3.08	13.62	8.66	0.15	0.12	64.82	49.46	0.19

and *Torodinium* sp.) to total microzooplankton biomass increased with temperature (r = 0.84; p < 0.05) from 3 to 40%. The relative biomass of heterotrophic taxa (including ciliates, dinoflagellates, and HNF) to total grazer biomass steadily increased with temperature >2°C (r = 0.83, p < 0.01). Mixotrophic chl *a* varied between 1.13 and 49.5% of total extracted chl *a* across the shelf (Table 2). Significantly higher values were measured within the PF (26.0 ± 12.5%) than in AW and the warmer NAW (7.36 ± 6.06 and 5.37 ± 5.21%, respectively).

Microbial food web dynamics

No nutrient-stimulated growth was observed for phytoplankton based on chl *a*, but picophytoplankton responded positively to fertilization in Expts 3, 8, 9, and 21. The chl-based phytoplankton growth rates (Fig. 3a) displayed strong seasonality (0.38–0.87 d^{-1} in May, 0.02–0.16 d^{-1} in June, and 0.03–0.55 d^{-1} in August and September), but no apparent temperature trend. No picophytoplankton growth was measured in AW incubations (with the exception of the PF in May, Expt 5, 0.44 d^{-1} at 0.27°C). In NAW, picophytoplankton growth rates were higher (*t*-test; p < 0.05) than those based on chl *a* (0.40 ± 0.20 d^{-1} and 0.19 ± 0.10 d^{-1}, respectively). Grazing mortality of phytoplankton (Fig. 3b) increased with temperature (r^2 = 0.69 and 0.48 for picoplankton and chl *a*, respectively; *t*-test, p < 0.005). Picoplanktivory was detectable even when the picoplankton numbers declined during AW incubations. The average grazing rate on the latter group exceeded that based on chl *a* in NAW (*t*-test, p < 0.05, 0.56 ± 0.28 and 0.28 ± 0.16 d^{-1}, respectively), whereas AW rates were similar (0.13 ± 0.06 and 0.19 ± 0.08 d^{-1}, respectively).

The proportion of heterotrophs in the total biomass of microbial grazers (i.e. microzooplankton plus

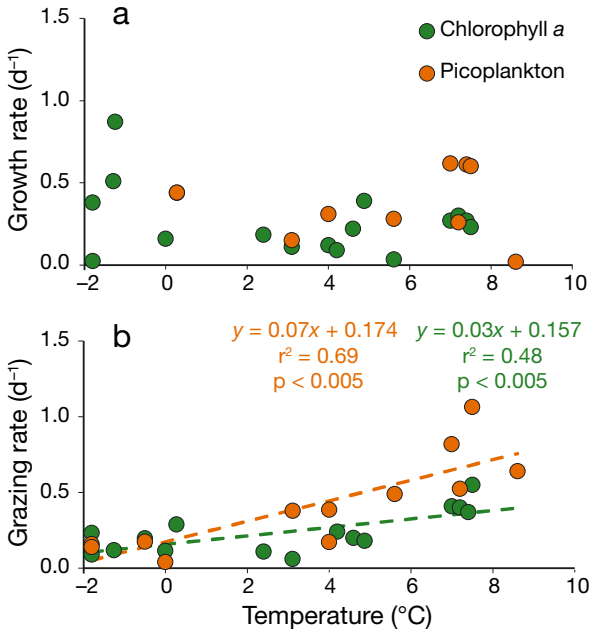

Fig. 3. (a) Growth and (b) grazing mortality rates of prey organisms in dilution experiments across a temperature gradient

HNF) correlated with herbivory rates across the temperature gradient (Fig. 4a). A similar relationship was found between herbivory and the relative biomass of microzooplankton cells <25 µm ESD (Fig. 4b). On average, grazers consumed, respectively, 15.5 ± 13.2% and 26.8 ± 20.9% chl *a* and picophytoplankton standing stocks daily (including 0 values). All of the above percentages were higher in NAW than AW, particularly at CW-affected stations. The percentage of chl *a* and picoplankton standing stocks removed by grazers increased with temperature (r = 0.68 and 0.87, respectively, p < 0.01). In addition, the percentage of primary production consumed (*g*:µ ratio) correlated with the percentage of growing microzooplankton (Fig. 4c).

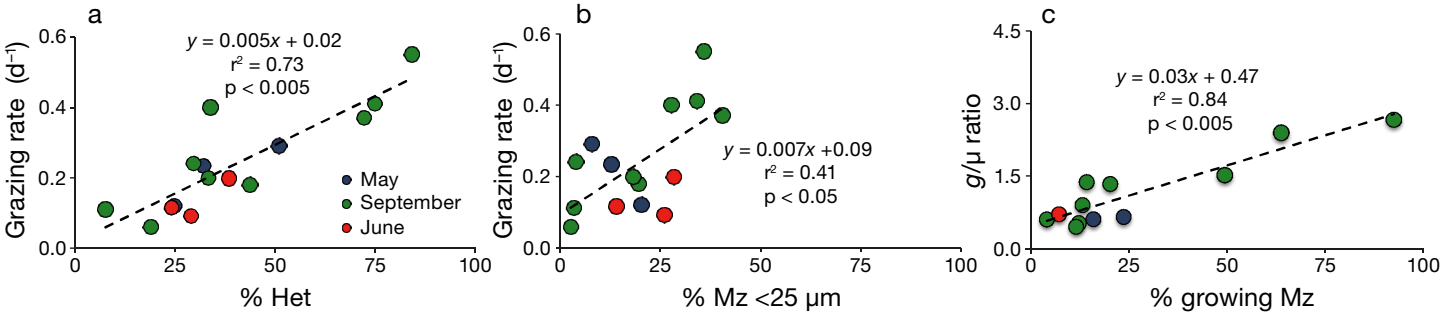

Fig. 4. Relationships between chlorophyll *a*-based herbivory rates and (a) the relative biomass of heterotrophs (% Het) and (b) the relative biomass of microzooplankton (Mz) <25 µm ESD (% Mz <25 µm). (c) Relationship between primary production consumed by Mz (*g*:µ ratio, where *g* is the grazing mortality rate and µ is phytoplankton growth) and the percentage of growing Mz

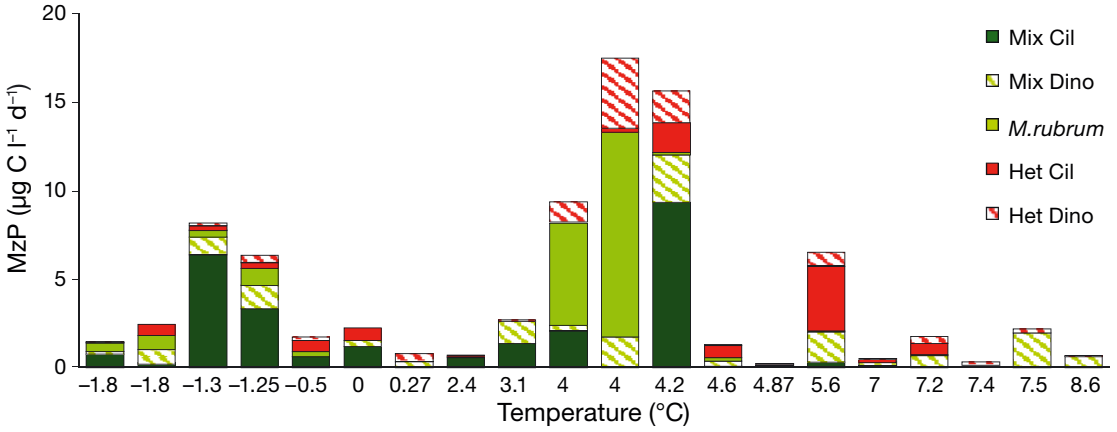

Fig. 5. Microzooplankton production (MzP, µg C l^{-1}) at different temperatures (note that data points from different locations/experiments may share the same ambient temperature). Abbreviations as in Fig. 2

Microzooplankton secondary production (MzP) varied from 0.15 to 17.5 µg C l^{-1} d^{-1} (Fig. 5), with maximum rates measured in NAW and the PF (17.5 and 15.6 µg C l^{-1} d^{-1} in June and August, respectively). The average rates were not statistically different between AW and NAW (2.85 ± 1.99 and 4.57 ± 5.97 µg C l^{-1} d^{-1}, respectively), resulting in a shelf-average of 3.96 ± 4.94 µg C l^{-1} d^{-1}, including 1.04 µg C l^{-1} d^{-1} due to *M. rubrum*. Production of the latter species peaked at 11.5 µg C l^{-1} d^{-1} in Expt 21. Ciliates contribution to MzP exceeded that of dinoflagellates in AW (69%) and was nearly equal in NAW (48%); mixotrophic taxa accounted for 74% of total MzP in AW. The proportion of heterotrophic taxa in MzP increased with temperature at nearly the same rate in AW and NAW (Fig. 6), with the exception of the 2 warmest stations (Expts 6 and 9), where mixotrophic dinoflagellates were responsible for almost all MzP. Between 0 and 5°C, MzP correlated with chl *a* (r = 0.80, p < 0.01).

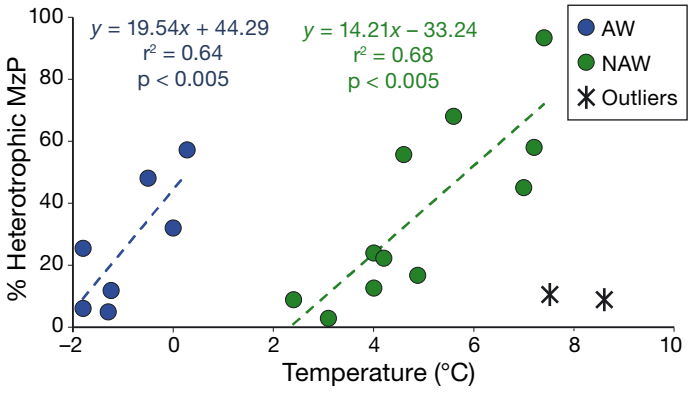

Fig. 6. Relationship between heterotrophic microzooplankton relative production (MzP) and temperature in Arctic Water (AW) and North Atlantic Water (NAW)

The ratios of MzP (without *M. rubrum*) to chl *a* and chl *a* consumed (µg C µg chl l^{-1} d^{-1}) were much higher in the PF and colder NAW than in AW and warmer NAW-CW (Fig. 7a). The first ratio, indicating the level of microzooplankton productivity relative to the concentration of their potential prey, correlated negatively with the relative biomass of grazers <25 µm ESD (Fig. 7b). The second ratio, indicating

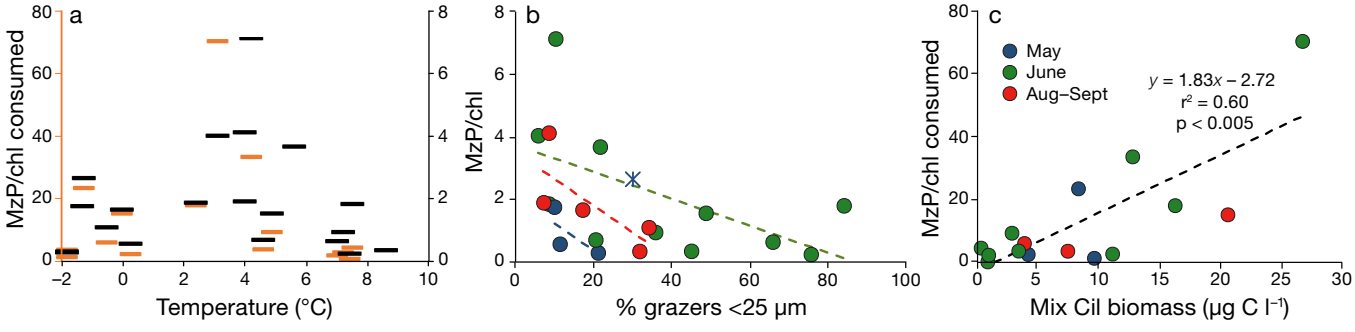

Fig. 7. Relationship (a) between the ratio of microzooplankton production (MzP) to chlorophyll *a* (chl *a*, orange dashes) and to chl *a* consumed (black dashes) and temperature, (b) between MzP/chl *a* and the percentage of grazers <25 µm ESD (including ciliates, dinoflagellates, and heterotrophic nanoflagellates [HNF]), and (c) between MzP/chl *a* consumed and the biomass of mixotrophic ciliates (Mix Cil)

the level of microzooplankton productivity relative to the consumed prey, increased with biomass of mixotrophic ciliates (Fig. 7c).

On average, the percentage of growing microzooplankton was 32 ± 23% and 33 ± 28% in AW and NAW, respectively. This proportion correlated with chl *a* ($r = 0.55$, $p < 0.05$) at chl *a* < 3 µg l^{-1}. The combined MzP:*B* ratio of growing populations varied between 0.22 and 0.94 (0.47 ± 0.19 shelf-wide). The rest of the microzooplankton either declined or, in many cases, did not change significantly during the 24 h incubations, resulting in the average community MzP:*B* ratio of 0.16 ± 0.14 (Table 2). The maximum ratio of 1.60 in Expt 9 (7.5°C) was due to the remarkably fast growth of mixotrophic dinoflagellates and was considered an outlier.

DISCUSSION

Temperature and food web structure

The dynamics of sea temperature and ice cover act as a pivot point through which changes in climatic patterns are translated to the marine ecosystems (Montoya & Raffaelli 2010). Bottom-up and top-down controls of microbial plankton will likely co-vary in response to these dominant abiotic factors. For example, phytoplankton composition plays a central role in determining microzooplankton composition (Caron & Hutchins 2013). Similar to the distribution patterns observed in this study, large ciliates and heterotrophic dinoflagellates usually form microzooplankton biomass (e.g. Lovejoy et al. 2002, Olson & Strom 2002, Sherr et al. 2013) and are the primary herbivores in diatom-dominated polar waters (Sherr et al. 2009, 2013). On the other hand, the higher contribution of small microzooplankton in NAW corresponded to an increase in microzooplankton picoplanktivory, which outpaced the temperature-driven increase in herbivory rates based on chl *a*.

Given tight trophic coupling between microzooplankton and planktonic copepods in the Arctic (Levinsen et al. 2000a, Campbell et al. 2009, Saiz et al. 2013), top-down control also appears to be a likely scenario, especially for NAW. The southern Barents Sea experiences large-scale advection of Atlantic zooplankton (Wassmann et al. 2015). The dominant Atlantic expatriate *Calanus finmarchicus* is an opportunistic omnivore that feeds on both phytoplankton and ciliates (Ohman & Runge 1994). Its Arctic congener *C. glacialis* exhibits similar feeding behavior (Levinsen et al. 2000a, Campbell et al. 2009). However, in the open Barents Sea waters dominated by small phytoplankton, large copepods are more likely to increase their reliance on microzooplankton for food (Wassmann et al. 2006b), raising the possibility of cascading effects in the microbial food web.

These intricately intertwined factors make it difficult to separate direct and indirect temperature effects in field experiments, particularly at the consumer level. Nevertheless, temperature was the only factor that consistently correlated with microbial parameters in this study. The effect of temperature on microzooplankton structure and dynamics was evident in August, when most stations were dominated by small phytoplankton. Further, changes in the microbial food web observed across the temperature gradient in the Barents Sea remained distinct when the data from all cruises were combined. This is remarkable given the pronounced seasonality in phytoplankton composition and productivity. The temperature-linked increase in bacterial biomass correspond well to temperature responses of bacterial production (Sturluson et al. 2008, Børsheim & Drinkwater 2014) and grazing mortality rates measured in the Barents Sea (Lara et al. 2013) and the adjacent Greenland Sea waters (Boras et al. 2010). Combined with the increased relative biomass of HNF and heterotrophic microzooplankton, it may indicate that more carbon is channeled through the microbial loop in warmer NAW. This trend appears to correspond to the results of the temperature-shift experiments mentioned earlier (Holding et al. 2013, Coello-Camba et al. 2015). However, no temperature thresholds in microbial dynamics or structure were apparent during our study ($H3_0$). These findings corroborate the conclusions of a recent modeling-mesocosm study in Kongsfjorden (Larsen et al. 2015), where a resilient microbial food web was found when plankton were allowed to adapt to temperature change.

Grazing rates

The observed increases in microzooplankton grazing rates and relative impacts with temperature support our *H*1 and correspond to the temperature–herbivory relationship reported from the Barents Sea earlier (Verity et al. 2002). Herbivory also correlated with the relative biomass of heterotrophic microzooplankton. Thus, our study appears to support the contention that heterotrophic plankton will respond to climate change faster than their autotrophic prey (Rose & Caron 2007). At the same time, Arctic protists

display broad thermal tolerance (Hansen et al. 1996, Levinsen et al. 1999, Franzè & Lavrentyev 2014). The practically overnight increase in temperature by 4.5°C in Expt 16 did not induce significant changes in microzooplankton production and feeding rates compared to other experiments at similar starting temperatures.

The g:μ ratios based on water mass means (including 0 values) indicate that grazing mortality and growth rates of phytoplankton were nearly balanced in the PF and NAW, whereas grazing exceeded phytoplankton growth in NAW-CW. In ice-covered waters, herbivores consumed 57% of daily phytoplankton production. Whether this difference was due to temperature, phytoplankton composition, or their combined effect, $H2$ is well supported by the obtained data. The resulting shelf-wide average of 92% corresponds to predictions that microzooplankton herbivory is a key factor in both diatom- (Hansen et al. 1996) and flagellate-dominated waters of the Barents Sea (Wassmann et al. 2006b). Combined with published data obtained in other parts of the Arctic (Table 3), these results also corroborate the idea that microzooplankton herbivory is a leading top-down control on phytoplankton growth in polar waters (Sherr et al. 2013).

Mixotrophy

Mixotrophy is prevalent in the Arctic, where plastidic ciliates form a large fraction of microzooplankton (Putt 1990, Levinsen et al. 2000b, Seuthe et al. 2011b, Stoecker et al. 2014b). The calculated contribution of mixotrophs to total chl *a* (Table 2) is significant, given that we collected our samples in the DCM, where phytoplankton peak in the water column. These estimates are likely conservative because the concentration of mixotrophic ciliates in the sub-surface layer was typically higher than in the DCM (P. Lavrentyev & G. Franzè unpublished data). In the Bering Sea, the calculated ciliate chl *a* was sometimes >50% of total chl *a* (Stoecker et al. 2014b). The chl *a* cellular quota calculated for the common oligotrich ciliate *Strombidium conicum* (30 000 μm^3, 55 pg chl cell^{-1}) in this study matched that measured directly in the Barents Sea (48 pg chl cell^{-1}, Putt 1990). However, oligotrich chl *a* content can be much higher (Stoecker et al. 1988, McManus et al. 2012).

In contrast to the receding ice-edge in spring, the Barents Sea PF does not stimulate phytoplankton productivity in summer (Reigstad et al. 2011, Erga et al. 2014). The elevated MzP:chl *a* ratio and the significant correlation between MzP and chl *a* in this region suggest some degree of food limitation. Under such conditions, mixotrophy can provide an advantage over strict heterotrophy. The same oligotrich species dominated summer microzooplankton in the Bering Sea (4–8°C, Stoecker et al. 2014b) and the Pechora and Kara Seas shelf (8–12°C, Lavrentyev 2012). Therefore, top-down pressure is the most plausible explanation for their sharp decline >5°C. In a companion study in the Barents Sea, mixotrophic ciliates were selectively grazed by copepods (P. J. Lavrentyev et al. unpubl.). Nevertheless, the increase in heterotrophic microzooplankton relative production with temperature in both AW and NAW leaves open the possibility of a direct temperature effect.

Table 3. Chlorophyll *a*-based phytoplankton growth (μ) and grazing mortality rates (g) and percentage of primary production consumed (% pPP) measured in dilution experiments in different Arctic and sub-Arctic seas; means ± SD; nd: no data

Region	Temp. (°C)	Chl (μg l^{-1})	μ (d^{-1})	g (d^{-1})	% pPP	Reference
Barents Sea	−1.6 to 7.4	0.66 ± 0.20	0.32 ± 0.13	0.24 ± 0.11	64 to 97	Verity et al. (2002)
Barents Sea	−1.8 to 8.9	1.70 ± 1.14	0.23 ± 0.22	0.18 ± 0.16	14 to >100	This study
Kara Sea and Yenisei Gulf	8.3 to 9.5	1.63 ± 1.31	0.43 ± 0.10	0.50 ± 0.06	85 to >100	Lavrentyev (2012)
Greenland Sea/Arctic Ocean	−1.5 to 7.5	3.62 ± 2.72	−0.04 ± 0.13	−0.09 ± 0.13	0	Calbet et al. (2011a)
W Greenland Sea	3.6 to 5.2	1.33 ± 0.56	−0.01 ± 0.16	0.12 ± 0.14	87 to >100	Calbet et al. (2011b)[a]
Baffin Bay and Jones Sound	nd	2.17 ± 2.68	0.21 ± 0.08	0.13 ± 0.03	36 to >100	Paranjape (1987)
Beaufort/Chukchi Sea	−1.7 to 5.2	2.61 ± 3.91	0.18 ± 0.13	0.05 ± 0.05	8 to >100	Sherr et al. (2009)[b]
SE Bering Sea	1.5 to 10.5	1.40 ± 1.10	0.53 ± 0.21	0.43 ± 0.28	31 to >100	Olson & Strom (2002)
SE Bering Sea	9.3 to 13.4	1.43 ± 1.02	0.34 ± 0.26	0.13 ± 0.08	3 to >100	Strom & Fredrickson (2008)
Bering Sea	−1.6 to 3.5	7.34 ± 9.20	0.20 ± 0.13	0.09 ± 0.10	26 to 86	Sherr et al. (2013)
E Bering Sea	2.3 to 7.9	0.59 ± 0.19	0.26 ± 0.09	0.24 ± 0.05	67 to >100	Stoecker et al. (2014a)

[a]Data from the inner fjord and glacier are not included
[b]Non-significant and negative rates are included as zero values

Microzooplankton production and microbial food web efficiency

To our knowledge, this is the first field study to experimentally examine polar microzooplankton productivity across a broad range of environmental conditions. The fact that only about a third of the community grew in any given experiment reflects asynchronicity in the growth of dominant species. Due to their competitive and/or predator–prey interactions, multiple populations comprising microzooplankton may oscillate out of phase, whereas short-term incubations provide only a snapshot of these dynamics. The correlation between the percentage of growing microzooplankton and the g:μ ratio indicates that microzooplankton growth has a direct effect on their trophic activities at the community level, even though growth and grazing may be decoupled short term at the population level.

The average daily MzP:B coefficient (0.16 ± 0.14, excluding the extreme value in Expt 9), combined with the average microzooplankton biomass of 1.0 g C m^{-2} in the Barents Sea (Rat'kova & Wassmann 2002, P. Lavrentyev & G. Franzè unpublished data), yields production of 24 g C m^{-2} for the growing season (May to September). This value is more than twice the combined annual copepod and krill production (~10 g C m^{-2} yr^{-1}, Sakshaug & Kovacs 2009) and ca. 23% of annual primary production in the Barents Sea (103 g C m^{-2} yr^{-1}, Ellingsen et al. 2008, Reigstad et al. 2011). These estimates are likely conservative. Microzooplankton survive through the long polar winter (Druzhkov & Druzhkova 1998, Møller et al. 2006), including mixotrophic oligotrichs and *Mesodinium rubrum* (Levinsen et al. 2000b), and increase rapidly in response to increased chl *a* in April (Levinsen et al. 2000b, Seuthe et al. 2011a).

The shelf-wide average MzP measured in the DCM during our study (2.93 ± 3.53 μg C l^{-1} d^{-1}, excluding *M. rubrum*) was similar to rates estimated for the marginal ice zone in the Barents Sea in spring (Hansen et al. 1996) and the ice-free Bering Sea in summer (Stoecker et al. 2014a). We calculated a microzooplankton ingestion rate (I) of 9.62 μg C l^{-1} d^{-1} based on the average chl *a* standing stock removal rate of 0.24 μg chl l^{-1} d^{-1} measured in this study and the phytoplankton C:chl *a* ratio of 40 in the DCM (Sakshaug et al. 2009). The resulting MzP:I ratio of 30% corresponds to the average gross growth efficiency commonly reported for zooplankton (Straile 1997). In the warm (>7°C) NAW-CW off the Finnmark coast, this ratio was considerably lower (6%). Given the increased contribution of HNF and smaller microzooplankton in these waters, it could indicate a multilevel microbial food web. Combined with mixotrophic bacterivory reported for *Micromonas* (Sanders & Gast 2012), the high rates of picoplanktivory may indicate the potential importance of carbon recovered through the microbial loop for microzooplankton in NAW. In AW, the MzP:I ratio was also relatively low (17%) compared to NAW, the PF, and Isfjorden (60, 72, and 59%, respectively). The elevated production:ingestion ratios are likely due to a high degree of mixotrophy among microzooplankton, since large mixotrophic ciliates can enhance the energy transfer efficiency through the pelagic food web (Stoecker et al. 2009).

CONCLUSIONS

Although the effects of temperature were confounded by seasonality and complex biotic interactions among plankton, we observed several distinct changes within the microbial food web across the temperature gradient: (1) the relative biomass and production of heterotrophic microzooplankton, as well as the relative biomass of small microzooplankton and heterotrophic nanoflagellates, increased with temperature; (2) the rates and relative impact of microzooplankton herbivory also increased with temperature; (3) microzooplankton removed a significant proportion of phytoplankton standing stock and primary production in NAW, their impact was lower but considerable in ice-covered AW; (4) mixotrophic ciliates made a large contribution to microzooplankton biomass and total chl *a*, particularly in the PF. Overall, microbial food web structure changed gradually in response to temperature and was characterized by tight trophic linkages within the dominant water masses in the Barents Sea.

The Barents Sea ecosystem is distinct from other polar systems because of its productivity and strong Atlantic influence (Hunt et al. 2013). However, the obtained data reveal a common pattern with other polar seas in that microzooplankton play a major role in the pelagic food web. The elevated role of microzooplankton has important implications for pelagic carbon flux in the Arctic. Primary production consumed by protists is channeled to mesozooplankton and remineralized in the water column. As microzooplankton do not produce rapidly sinking fecal pellets (some even feed on copepod fecal pellets, Svensen et al. 2012), the net effect is carbon retention in the mixed layer. Thus, the elevated role of microbial plankton in an ice-free Arctic may benefit the pelagic

food web (e.g. Levinsen et al. 2000a) and lead to weaker pelagic–benthic coupling (Kedra et al. 2015) and decreased benthic secondary production (Degen et al. 2016). Given the scale of carbon flux through microzooplankton, including mixotrophy, this critical pelagic food web component must be incorporated into models predicting the potential effects of climate change on polar marine ecosystems.

Acknowledgements. This study was supported by the National Science Foundation (Award ARC-0909372). We thank Paul Wassmann, Marit Reigstad, Lena Seuthe, Camilla Svensen, Jostein Røttingen, Francisco Moore, Konstantin Solovyev, and the captains and crews of RVs 'Helmer Hanssen' (formerly 'Jan Mayen') and 'G.O. Sars' for their logistical support and field assistance, and to Barry and Evelyn Sherr and Diane Stoecker for data sharing.

LITERATURE CITED

Anderson MR, Rivkin RB (2001) Seasonal patterns in grazing mortality of bacterioplankton in polar oceans: a bipolar comparison. Aquat Microb Ecol 25:195–206

Arrigo KR, van Dijken GL (2011) Secular trends in Arctic Ocean net primary production. J Geophys Res 116: C09011

Arthun M, Eldevik T, Smedsrud LH, Skagseth O, Ingvaldsen RB (2012) Quantifying the influence of Atlantic heat on Barents Sea ice variability and retreat. J Clim 25: 4736–4743

Boitsov VD, Karsakov AL, Trofimov AG (2012) Atlantic water temperature and climate in the Barents Sea, 2000-2009. ICES J Mar Sci 69:833–840

Boras JA, Montserrat Sala M, Arrieta JM, Sà EL and others (2010) Effect of ice melting on bacterial carbon fluxes channelled by viruses and protists in the Arctic Ocean. Polar Biol 33:1695–1707

Børsheim KY, Drinkwater KF (2014) Different temperature adaptation in Arctic and Atlantic heterotrophic bacteria in the Barents Sea Polar Front region. J Mar Syst 130: 160–166

Brown ZW, Arrigo KR (2012) Contrasting trends in sea ice and primary production in the Bering Sea and Arctic Ocean. ICES J Mar Sci 69:1180–1193

Calbet A, Landry MR (2004) Phytoplankton growth, microzooplankton grazing, and carbon cycling in marine systems. Limnol Oceanogr 49:51–57

Calbet A, Saiz E (2013) Effects of trophic cascades in dilution grazing experiments: from artificial saturated feeding responses to positive slopes. J Plankton Res 35: 1183–1191

Calbet A, Saiz E, Almeda R, Movilla JI, Alcaraz M (2011a) Low microzooplankton grazing rates in the Arctic Ocean during a *Phaeocystis pouchetii* bloom (Summer 2007): fact or artifact of the dilution technique? J Plankton Res 33:687–701

Calbet A, Riisgaard K, Saiz E, Zamora S, Stedmon C, Nielsen TG (2011b) Phytoplankton growth and microzooplankton grazing along a sub-Arctic fjord (Godthåbsfjord, west Greenland). Mar Ecol Prog Ser 442:11–22

Campbell RG, Sherr EB, Ashjian CJ, Plourde S, Sherr BF, Hill V, Stockwell DA (2009) Mesozooplankton prey preference and grazing impact in the western Arctic Ocean. Deep Sea Res II 56:1274–1289

Caron DA, Hutchins DA (2013) The effects of changing climate on microzooplankton grazing and community structure: drivers, predictions and knowledge gaps. J Plankton Res 35:235–252

Chen B, Landry MR, Huang B, Liu H (2012) Does warming enhance the effect of microzooplankton grazing on marine phytoplankton in the ocean? Limnol Oceanogr 57: 519–526

Coello-Camba A, Agusti S, Vaque D, Holding J, Arrieta JM, Wassmann P, Duarte CM (2015) Experimental assessment of temperature thresholds for Arctic phytoplankton communities. Estuaries Coasts 38:873–885

Degen R, Jørgensen LL, Ljubin P, Ellingsen IH, Pehlke H, Brey T (2016) Patterns and drivers of megabenthic secondary production on the Barents Sea shelf. Mar Ecol Prog Ser 546:1–16

Dolan JR, Perez MT (2000) Costs, benefits and characteristics of mixotrophy in marine oligotrichs. Freshw Biol 45: 227–238

Dolan JR, Gallegos CL, Moigis A (2000) Dilution effects on microzooplankton in dilution grazing experiments. Mar Ecol Prog Ser 200:127–139

Druzhkov NV, Druzhkova EI (1998) Microzooplankton in the Pechora and Kara Seas in the end of winter. In: Matishov GG (ed) Biology and oceanography of the Kara and Barents Seas (along the Northeast Passage). Russian Academy Sciences, Apatity, p 120–138

Druzhkova EI, Makarevich PR (2008) Annual cycle of nanophytoplankton in coastal waters of the Barents Sea. Izv Akad Nauk Ser Biol 35:428–435

Ellingsen IH, Dalpadado P, Slagstad D, Loeng H (2008) Impact of climatic change on the biological production in the Barents Sea. Clim Change 87:155–175

Erga SR, Ssebiyonga N, Hamre B, Frette Ø and others (2014) Environmental control of phytoplankton distribution and photosynthetic performance at the Jan Mayen Front in the Norwegian Sea. J Mar Syst 130:193–205

First MR, Lavrentyev PJ, Jochem FJ (2007) Patterns of microzooplankton growth in dilution experiments across a trophic gradient: implications for herbivory studies. Mar Biol 151:1929–1940

Franzè G, Lavrentyev PJ (2014) Microzooplankton growth rates examined across a temperature gradient in the Barents Sea. PLOS ONE 9:e86429

Garcia-Cuetos L, Moestrup O, Hansen PJ (2012) Studies on the genus *Mesodinium*: II. Ultrastructural and molecular investigations of five marine species help clarifying the taxonomy. J Eukaryot Microbiol 59:374–400

Gifford DJ (1985) Laboratory culture of marine planktonic oligotrichs (Ciliophora, Oligotrichida). Mar Ecol Prog Ser 23:257–267

Hansen B, Christiansen S, Pedersen G (1996) Plankton dynamics in the marginal ice zone of the central Barents Sea during spring: carbon flow and structure of the grazer food chain. Polar Biol 16:115–128

Holding JM, Duarte CM, Arrieta JM, Vaquer-Sunyer R, Coello-Camba A, Wassmann P, Agusti S (2013) Experimentally determined temperature thresholds for Arctic plankton community metabolism. Biogeosciences 10: 357–370

Howard-Jones MH, Ballard VD, Allen AE, Frischer ME, Verity PG (2002) Distribution of bacterial biomass and activ-

ity in the marginal ice zone of the central Barents Sea during summer. J Mar Syst 38:77–91
Hunt GL Jr, Blanchard AL, Boveng P, Dalpadado P and others (2013) The Barents and Chukchi Seas: comparison of two Arctic shelf ecosystems. J Mar Syst 109–110:43–68
Jakobsen HH, Carstensen J (2011) FlowCAM: sizing cells and understanding the impact of size distributions on biovolume of planktonic community structure. Aquat Microb Ecol 65:75–87
Kedra M, Moritz C, Choy ES, David C and others (2015) Status and trends in the structure of Arctic benthic food webs. Polar Res 34:23775
Kirchman DL, Moran XA, Ducklow H (2009) Microbial growth in the polar oceans — role of temperature and potential impact of climate change. Nat Rev Microbiol 7: 451–459
Kwok R, Rothrock DA (2009) Decline in Arctic sea ice thickness from submarine and ICESat records: 1958–2008. Geophys Res Lett 36:L15501
Landry MR, Brown SL, Yoshimi MR, Selph KE, Bidigare RR, Yang EJ, Simmons MP (2008) Depth-stratified phytoplankton dynamics in Cyclone Opal, a subtropical mesoscale eddy. Deep-Sea Res II 55:1348–1359
Lara E, Arrieta JM, Garcia-Zarandona I, Boras JA and others (2013) Experimental evaluation of the warming effect on viral, bacterial and protistan communities in two contrasting Arctic systems. Aquat Microb Ecol 70:17–32
Larsen A, Egge JK, Nejstgaard JC, Di Capua I, Thyrhaug R, Bratbak G, Thingstad TF (2015) Contrasting response to nutrient manipulation in Arctic mesocosms are reproduced by a minimum microbial food web model. Limnol Oceanogr 60:360–374
Lavrentyev PJ (2012) Microzooplankton studies in the Kara Sea during the Yamal-Arctic 2012 expedition. Russ Polar Res 10:24–26 (in Russian)
Levinsen H, Nielsen TG, Hansen BW (1999) Plankton community structure and carbon cycling on the western coast of Greenland during the stratified summer situation. II. Heterotrophic dinoflagellates and ciliates. Aquat Microb Ecol 16:217–232
Levinsen H, Turner JT, Nielsen TG, Hansen BW (2000a) On the trophic coupling between protists and copepods in arctic marine ecosystems. Mar Ecol Prog Ser 204:65–77
Levinsen H, Nielsen TG, Hansen BW (2000b) Annual succession of marine pelagic protozoans in Disko Bay, West Greenland, with emphasis on winter dynamics. Mar Ecol Prog Ser 206:119–134
Li WKW, McLaughlin FA, Lovejoy C, Carmack EC (2009) Smallest algae thrive as the Arctic Ocean freshens. Science 326:539
Loeng H (1991) Features of the physical oceanographic conditions of the Barents Sea. Polar Res 10:5–18
Lovejoy C, Legendre L, Price NM (2002) Prolonged diatom blooms and microbial food web dynamics: experimental results from an Arctic polynya. Aquat Microb Ecol 29: 267–278
Marie D, Partensky F, Jacquet S, Vaulot D (1997) Enumeration and cell cycle analysis of natural populations of marine picoplankton by flow cytometry using the nucleic acid stain SYBR Green I. Appl Environ Microbiol 63: 186–193
McBride MM, Dalpadado P, Drinkwater KF, Godø OR and others (2014) Krill, climate, and contrasting future scenarios for Arctic and Antarctic fisheries. ICES J Mar Sci 71:1934–1955
McManus GB, Schoener DM, Haberlandt K (2012) Chloroplast symbiosis in a marine ciliate: ecophysiology and the risks and rewards of hosting foreign organelles. Front Microbiol 3:321
Menden-Deuer S, Lessard EJ (2000) Carbon to volume relationships for dinoflagellates, diatoms, and other protist plankton. Limnol Oceanogr 45:569–579
Møller EF, Nielsen TG, Richardson K (2006) The zooplankton community in the Greenland Sea: composition and role in carbon turnover. Deep-Sea Res I 53:76–93
Montagnes DJS, Berges JA, Harrison PJ, Taylor FJR (1994) Estimating carbon, nitrogen, protein, and chlorophyll *a* from volume in marine-phytoplankton. Limnol Oceanogr 39:1044–1060
Montoya JM, Raffaelli D (2010) Climate change, biotic interactions and ecosystem services. Philos Trans R Soc Lond B Biol Sci 365:2013–2018
Nelson RJ, Ashjian CJ, Bluhm BA, Conlan KE and others (2014) Biodiversity and biogeography of the lower trophic taxa of the Pacific Arctic region: sensitivities to climate change. In: Grebmeier JM, Maslowski W (eds) The Pacific Arctic region: ecosystem status and trends in a rapidly changing environment. Springer, Dordrecht, p 269–336
Nielsen TG, Kiørboe T (1994) Regulation of zooplankton biomass and production in a temperate, coastal ecosystem. 2. Ciliates. Limnol Oceanogr 39:508–519
Nikiforov EG, Shpaikher AO (1980) Patterns of large-scale variability in the hydrological cycle of the Arctic Ocean. Hydrometizdat, Leningrad (in Russian)
Norland S (1993) The relationship between biomass and volume of bacteria. In: Kemp PF, Sherr EB, Sherr BF, Cole JJ (eds) Handbook of methods in aquatic microbial ecology. CRC Press, Boca Raton, FL, p 303–308
Not F, Massana R, Latasa M, Marie D and others (2005) Late summer community composition and abundance of photosynthetic picoeukaryotes in Norwegian and Barents Seas. Limnol Oceanogr 50:1677–1686
Ohman MD, Runge JA (1994) Sustained fecundity when phytoplankton resources are in short supply: omnivory by *Calanus finmarchicus* in the Gulf of St-Lawrence. Limnol Oceanogr 39:21–36
Olson MB, Strom SL (2002) Phytoplankton growth, microzooplankton herbivory and community structure in the southeast Bering Sea: insight into the formation and temporal persistence of an *Emiliania huxleyi* bloom. Deep-Sea Res II 49:5969–5990
Paranjape MA (1987) Grazing by microzooplankton in the eastern Canadian arctic in summer 1983. Mar Ecol Prog Ser 40:239–246
Polyakov IV, Timokhov LA, Alexeev VA, Bacon S and others (2010) Arctic Ocean warming contributes to reduced polar cap. J Phys Oceanogr 40:2743–2756
Porter KG, Feig YS (1980) The use of DAPI for identifying and counting aquatic microflora. Limnol Oceanogr 25: 943–948
Putt M (1990) Abundance, chlorophyll content and photosynthetic rates of ciliates in the Nordic Seas during summer. Deep-Sea Res I 37:1713–1731
Putt M, Stoecker DK (1989) An experimentally determined carbon:volume ratio for marine oligotrichous ciliates from estuarine and coastal waters. Limnol Oceanogr 34: 1097–1103
Qu B, Gabric AJ, Matrai PA (2006) The satellite-derived distribution of chlorophyll-a and its relation to ice cover,

radiation and sea surface temperature in the Barents Sea. Polar Biol 29:196–210

Rat'kova TN, Wassmann P (2002) Seasonal variation and spatial distribution of phyto- and protozooplankton in the central Barents Sea. J Mar Syst 38:47–75

Reigstad M, Carroll J, Slagstad D, Ellingsen IH, Wassmann P (2011) Intra-regional comparison of productivity, carbon flux and ecosystem composition within the northern Barents Sea. Prog Oceanogr 90:33–46

Rose JM, Caron DA (2007) Does low temperature constrain the growth rates of heterotrophic protists? Evidence and implications for algal blooms in cold waters. Limnol Oceanogr 52:886–895

Rose JM, Fitzpatrick E, Wang AN, Gast RJ, Caron DA (2013) Low temperature constrains growth rates but not short-term ingestion rates of Antarctic ciliates. Polar Biol 36: 645–659

Saiz E, Calbet A, Isari S, Antó M and others (2013) Zooplankton distribution and feeding in the Arctic Ocean during a *Phaeocystis pouchetii* bloom. Deep-Sea Res I 72:17–33

Sakshaug E, Kovacs KM (2009) Introduction. In: Sakshaug E, Johnsen GH, Kovacs KM (eds) Ecosystem Barents Sea. Tapir Academic Press, Trondheim, p 9–32

Sakshaug E, Johnsen G, Kristansen S, von Quillfeldt C, Rey F, Slagstad D, Thingstad F (2009) Phytoplankton and primary production. In: Sakshaug E, Johnsen GH, Kovacs KM (eds) Ecosystem Barents Sea. Tapir Academic Press, Trondheim, p 167–208

Sanders RW, Gast RJ (2012) Bacterivory by phototrophic picoplankton and nanoplankton in Arctic waters. FEMS Microbiol Ecol 82:242–253

Sarmento H, Montoya JM, Vazquez-Dominguez E, Vaque D, Gasol JM (2010) Warming effects on marine microbial food web processes: How far can we go when it comes to predictions? Philos Trans R Soc Lond B Biol Sci 365: 2137–2149

Seuthe L, Rokkan Iversen K, Narcy F (2011a) Microbial processes in a high-latitude fjord (Kongsfjorden, Svalbard): II. Ciliates and dinoflagellates. Polar Biol 34:751–766

Seuthe L, Töpper B, Reigstad M, Thyrhaug R, Vaquer-Sunyer R (2011b) Microbial communities and processes in ice-covered Arctic waters of the northwestern Fram Strait (75 to 80° N) during the vernal pre-bloom phase. Aquat Microb Ecol 64:253–266

Sherr EB, Sherr BF, Hartz AJ (2009) Microzooplankton grazing impact in the Western Arctic Ocean. Deep-Sea Res II 56:1264–1273

Sherr EB, Sherr BF, Ross C (2013) Microzooplankton grazing impact in the Bering Sea during spring sea ice conditions. Deep-Sea Res II 94:57–67

Sieracki CK, Sieracki ME, Yentsch CS (1998) An imaging-in-flow system for automated analysis of marine microplankton. Mar Ecol Prog Ser 168:285–296

Slagstad D, Ellingsen IH, Wassmann P (2011) Evaluating primary and secondary production in an Arctic Ocean void of summer sea ice: an experimental simulation approach. Prog Oceanogr 90:117–131

Smolyar I, Adrov N (2003) The quantitative definition of the Barents Sea Atlantic Water: mapping of the annual climatic cycle and interannual variability. ICES J Mar Sci 60:836–845

Stocker TF, Qin D, Plattner GK, Tignor M and others (eds) (2013) Climate change 2013: the physical science basis. Contribution of Working Group I to the Fifth Assessment Report of the Intergovernmental Panel on Climate Change. Cambridge University Press, Cambridge and New York, NY

Stoecker DK, Silver MW, Michaels AE, Davis LH (1988) Obligate mixotrophy in *Laboea strobila*, a ciliate which retains chloroplasts. Mar Biol 99:415–423

Stoecker DK, Johnson MD, de Vargas C, Not F (2009) Acquired phototrophy in aquatic protists. Aquat Microb Ecol 57:279–310

Stoecker DK, Weigel A, Goes JI (2014a) Microzooplankton grazing in the Eastern Bering Sea in summer. Deep-Sea Res II 109:145–156

Stoecker DK, Weigel AC, Stockwell DA, Lomas MW (2014b) Microzooplankton: abundance, biomass and contribution to chlorophyll in the Eastern Bering Sea in summer. Deep-Sea Res II 109:134–144

Straile D (1997) Gross growth efficiencies of protozoan and metazoan zooplankton and their dependence on food concentration, predator-prey weight ratio, and taxonomic group. Limnol Oceanogr 42:1375–1385

Strom SL, Fredrickson KA (2008) Intense stratification leads to phytoplankton nutrient limitation and reduced microzooplankton grazing in the southeastern Bering Sea. Deep Sea Res II 55:1761–1774

Sturluson M, Nielsen TG, Wassmann P (2008) Bacterial abundance, biomass and production during spring blooms in the northern Barents Sea. Deep-Sea Res II 55: 2186–2198

Svensen C, Riser CW, Reigstad M, Seuthe L (2012) Degradation of copepod faecal pellets in the upper layer: role of microbial community and *Calanus finmarchicus*. Mar Ecol Prog Ser 462:39–49

Tatters AO, Roleda MY, Schnetzer A, Fu F and others (2013) Short- and long-term conditioning of a temperate marine diatom community to acidification and warming. Philos Trans R Soc Lond B Biol Sci 368:20120437

Vage S, Basedow SL, Tande KS, Zhou M (2014) Physical structure of the Barents Sea Polar Front near Storbanken in August 2007. J Mar Syst 130:256–262

Verity PG, Wassmann P, Frischer ME, Howard-Jones MH, Allen AE (2002) Grazing of phytoplankton by microzooplankton in the Barents Sea during early summer. J Mar Syst 38:109–123

Wassmann P, Lenton TM (2012) Arctic tipping points in an Earth System perspective. Ambio 41:1–9

Wassmann P, Reigstad M (2011) Future Arctic Ocean seasonal ice zones and implications for pelagic-benthic coupling. Oceanography 24:220–231

Wassmann P, Slagstad D, Riser CW, Reigstad M (2006a) Modelling the ecosystem dynamics of the Barents Sea including the marginal ice zone. J Mar Syst 59:1–24

Wassmann P, Reigstad M, Haug T, Rudels B and others (2006b) Food webs and carbon flux in the Barents Sea. Prog Oceanogr 71:232–287

Wassmann P, Kosobokova KN, Slagstad D, Drinkwater KF and others (2015) The contiguous domains of Arctic Ocean advection: trails of life and death. Prog Oceanogr 139:42–65

Welschmeyer NA (1994) Fluorometric analysis of chlorophyll a in the presence of chlorophyll b and pheopigments. Limnol Oceanogr 39:1985–1992

Editorial responsibility: Sigrun Jónasdóttir, Charlottenlund, Denmark

Submitted: July 18, 2016; Accepted: January 31, 2017
Proofs received from author(s): March 22, 2017